12.007 Geobiology
Spring 2009

Geobiology 2009 Lecture 10
The Antiquity of Life on Earth

Homework #5

Topics (choose 1): Describe criteria for biogenicity in microscopic fossils. How do the oldest describes fossils compare? Use this to argue one side of the Brasier-Schopf debate

OR

What are stromatolites; where are they found and how are they formed? Articulate the two sides of the debate on antiquity and biogenicity.
Up to 4 pages, including figures.

Due 3/31/2009

Need to know

- How C and S- isotopic data in rocks are informative about the advent and antiquity of biogeochemical cycles
- Morphological remains and the antiquity of life; how do we weigh the evidence?
- Indicators of changes in atmospheric pO_2
- A general view of the course of oxygenation of the atm-ocean system

Readings for this lecture

Schopf J.W. et al., (2002) Laser Raman Imagery of Earth's earliest fossils. Nature 416, 73.

Brasier M.D. et al., (2002) Questioning the evidence for Earth's oldest fossils. Nature 416, 76.

Garcia-Ruiz J.M., Hyde S.T., Carnerup A. M. , Christy v, Van Kranendonk M. J. and Welham N. J. (2003) Self-Assembled Silica-Carbonate Structures and Detection of Ancient Microfossils Science 302, 1194-7.

Hofmann, H.J., Grey, K., Hickman, A.H., and Thorpe, R. 1999. Origin of 3.45 Ga coniform stromatolites in Warrawoona Group, Western Australia.
Geological Society of America, Bulletin, v. 111 (8), p. 1256-1262.

Allwood et al., (2006) Stromatolite reef from the Early Archaean era of Australia. Nature 441|, 714

J. William Schopf, Fossil evidence of Archaean life (2006) Phil. Trans. R. Soc. B 361, 869–885.

Martin Brasier, Nicola McLoughlin, Owen Green and David Wacey (2006) A fresh look at the fossil evidence for early Archaean cellular life. Phil. Trans. R. Soc. B 361, 887–902

Nature and Habitats of Early Life

- Evidence for Earth's earliest life forms and validity of that evidence
  - Stable isotopic tracers especially C & S
  - Microfossils
  - Stromatolites

- Facts about redox couples
- Consequences of oxygenic photosynthesis? Respiration
- Early record of preserved organic carbon and carbon isotopes
- Early record of molecular oxygen in the environment

- The Earliest Biogeochemical Cycles

Oldest Microfossils on Earth?

Warrawoona Group, N. Pole Dome/ Marble Bar, WA; 3.5 Ga

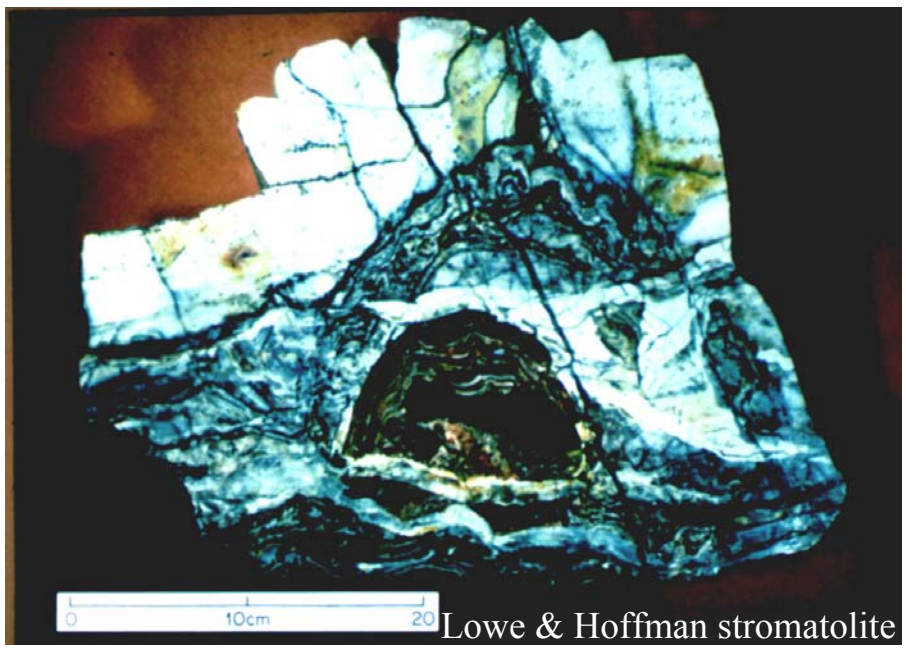

Lowe & Hoffman stromatolite

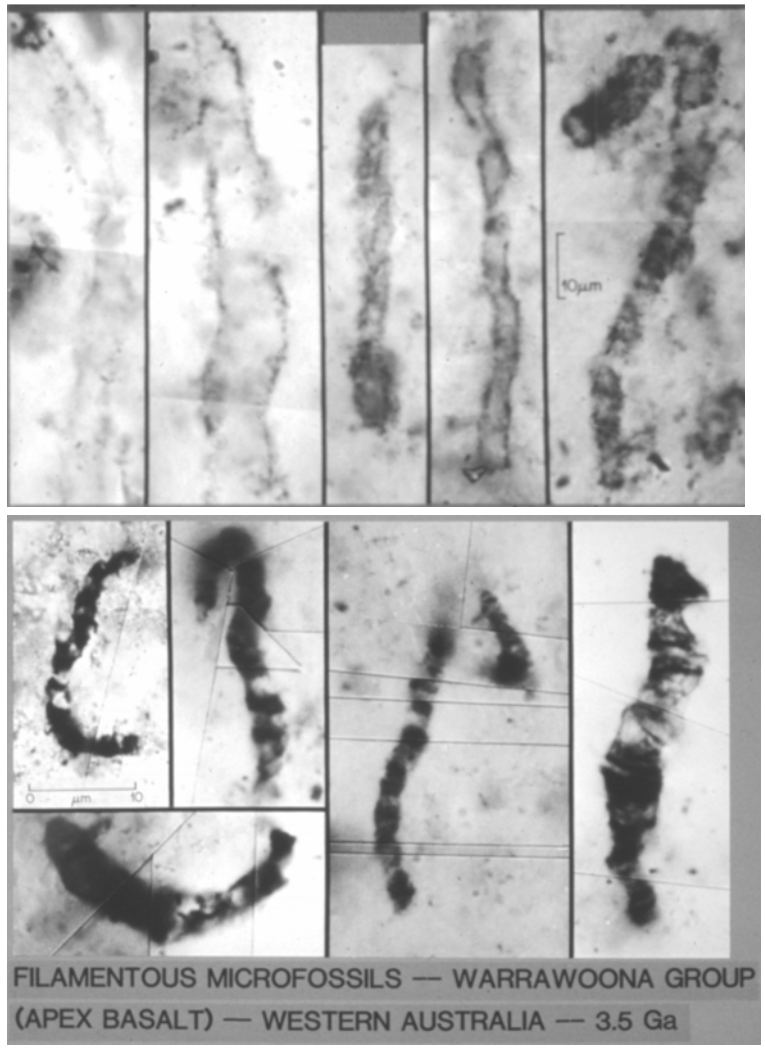

Courtesy Joe Kirschvink, CalTech

3.5-2.3 Ga Pilbara Craton, NW Australia

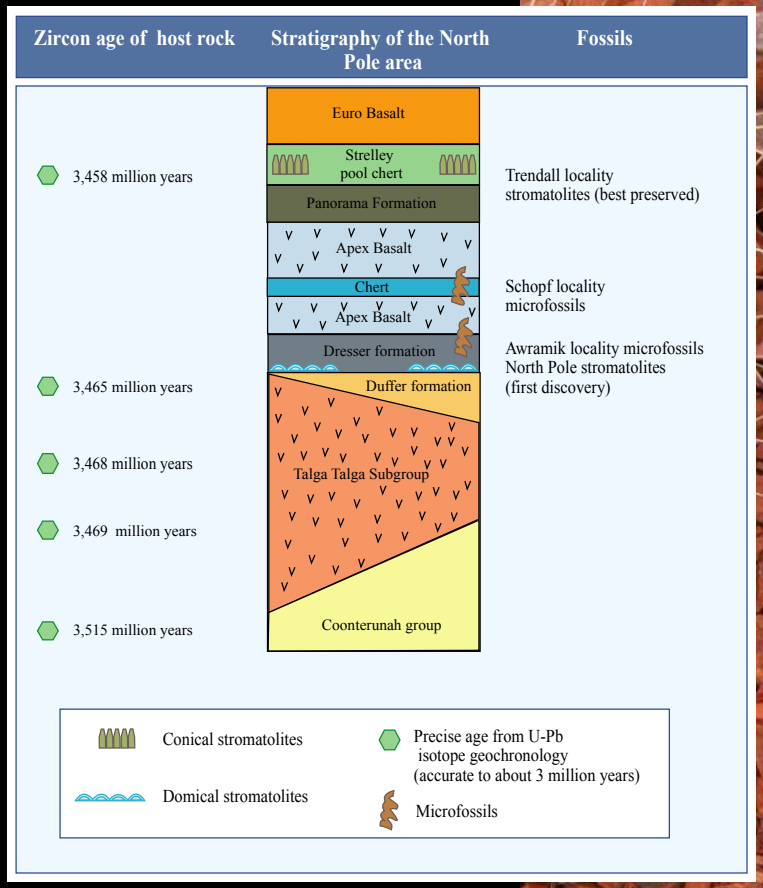

Figure by MIT OpenCourseWare.

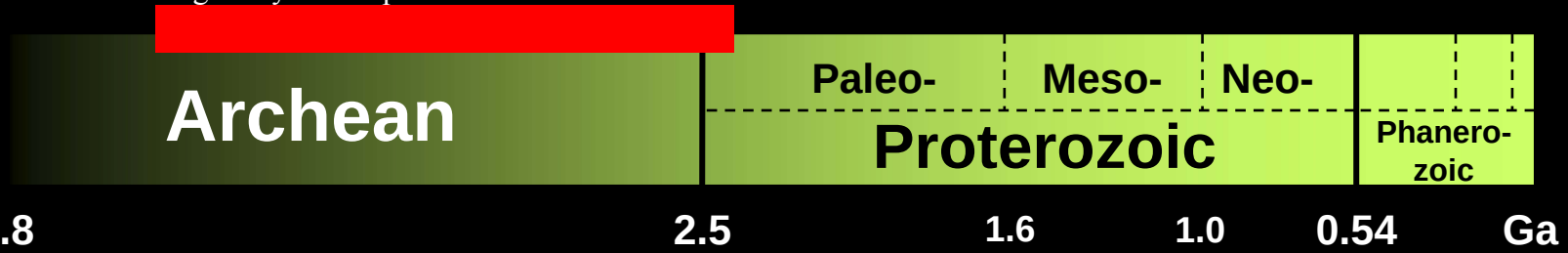


black chert veins and clasts
Complex 'Dyke' Breccia

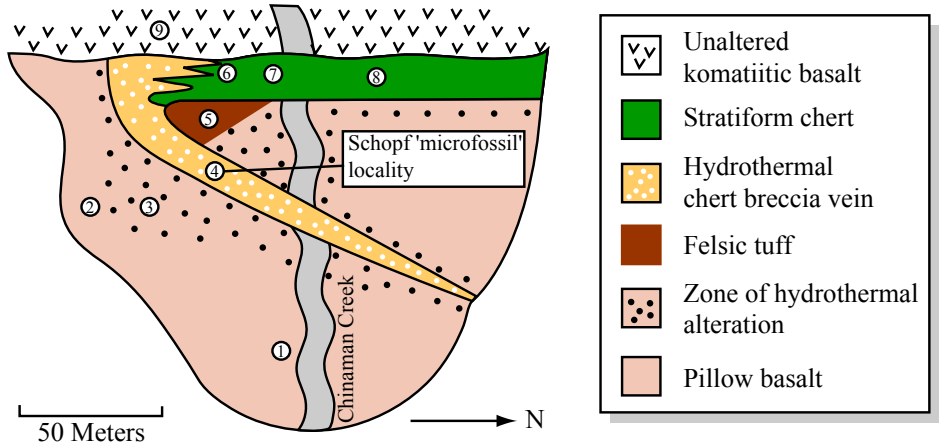

	1	2	3	4 A1/B1	4 A2/B2	4 A3/B3	4 C/A4	5	6	7	8	9
Chromite	–	–	–	●	●	■	–	●■	–	–	–	–
Iron oxide	■	■□	■	●	●	●■	–	●■	■	–	–	■□
TiO_2	■	■	–	●	●■	●■	–	●■□	–	–	■	■□
$BaSO_4$	–	□	–	●■	●■	●■	■□	■○□	●■	■○	■○	–
Alunite-jarosite	–	–	–	●■	●■	●■	■□	–	■*	●■*	●■○*	–
Aluminosilicates	■	■	■	●■	●■	●■	–	●■○	–	–	–	■□
Metals, *sulphides*	*Cu* ■	Ni □ Cu □ Zn □ Pb □	–	Fe ● Ni ● Cu ● Zn ● *Pb* ●	Fe ●■ *Fe* ●■ Ni ● Cu ● Zn ● Sn ● *Pb* ●	Fe ■ *Fe* ■ Cu ●	*Pb* □	Pb ●	*Fe* ■ *Cu* ■ Zn ■	*Fe* ●■ *Ni,As* □ *Cu* ●■ *Cu* ○□	Fe ■ *Fe* ●○ *Cu* ■ *Zn* ●○ *Zn* ■□ *Sb* ●○ *Sb* ■□	–
Sulphur (p.p.m.)				–	162	79			–	330	607	
Graphite				●■	●■	●■		●○■	●	●	●■○	
Carbon (p.p.m.)				126-1206	1413	36			34	2545	2162	
$\delta^{13}C_{PDB}$(%)				-30.3 -26.5	-29.9	-28.4			-25.6	-29.5	-25.6	
$\delta^{18}O_{SMOW}$(‰)				+14.5 +14.7	+14.5	+14.6 +14.7			+14.3	+14.1	+13.7	

● In shards, clasts ○ Around shards, clasts ■ In matrix □ In veins
* Arsenic-rich
A-C, Fabrics recognized in thin section Open box, not analysed

Figure by MIT OpenCourseWare. After Brasier et al., 2002.


Stephen Hyde

WARRAWOONA PROKARYOTIC MICROFOSSIL PILBARA CRATON WA ~ 3.5 Ga (J.W. SCHOPF, 1983)

Image removed due to copyright restrictions.

Image of the original Warrawoona microfossil (J.W. Schopff, 1983).

What Constitutes Compelling Evidence?

- Geologic source of material and probable age limits well-defined… eg pedigree and a sediment and not an igneous rock!
- Provenance of several comparably-aged assemblages similarly well established
- Fossils demonstrably indigenous to, and syngenetic, with deposition
- Demonstrably biogenic
  - ‘biological’ size distribution
  - morphologically comparable to specific modern taxa

from: Schopf, Hayes and Walter, Ch 15 Earth’s Earliest Biosphere, 1983

Text and image removed due to copyright restrictions.
Abstract and Fig. 2 in Brasler, Martin D., et al. "Questioning the Evidence for Earth's Oldest Fossils." *Nature* 416 (2002): 76-81.

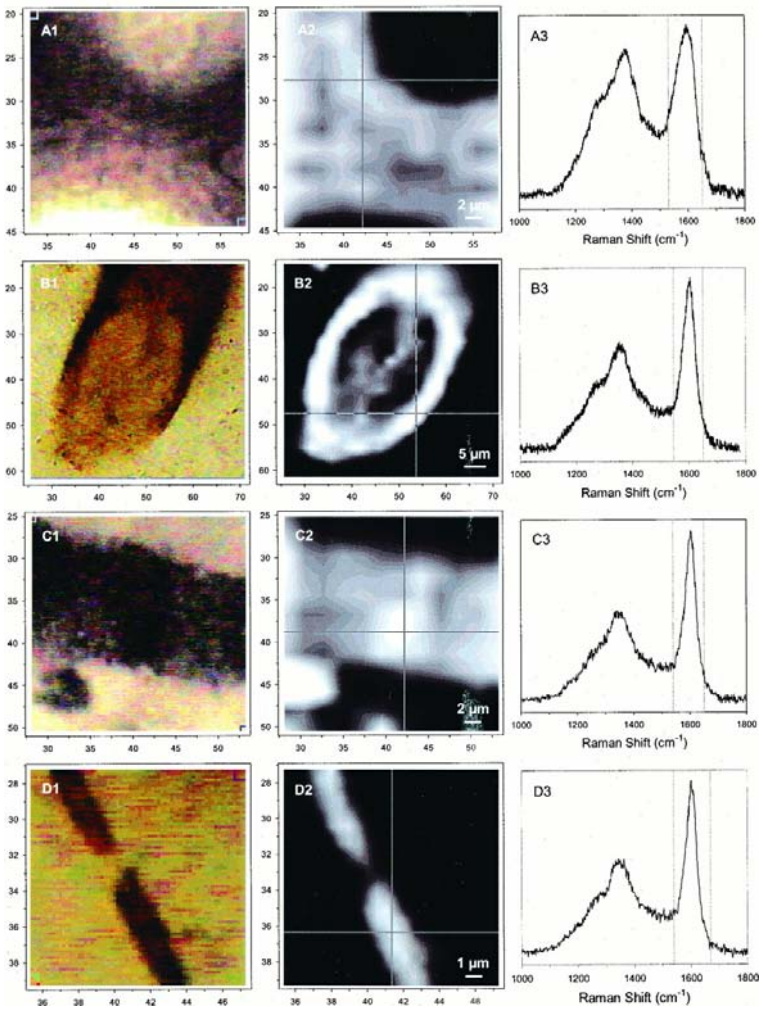

Kudryavtsev, Anatoliy B. et al. (2001) Proc. Natl. Acad. Sci. USA 98, 823-826

Courtesy of National Academy of Sciences, U. S. A. Used with permission. Source: Kudryavtsev, Anatoliy B., J. William Schopf, David G. Agresti, and Thomas J. Wdowiak. "In Situ Laser-Raman Imagery of Precambrian Microscopic Fossils." *PNAS* 98 (2001): 823-826. (c) 2001 National Academy of Sciences, U.S.A.

Fig. 1. Optical images (column 1), Raman images (column 2), and spectral bands used for Raman imaging (column 3) of permineralized carbonaceous fossils at or near the upper surfaces of polished chert thin sections: (*A*) Cell wall in the conductive tissue (lignified xylem) of an aquatic fern cf. *Dennstaedtia* from the essentially unmetamorphosed 45-Ma-old Clarno Formation of Oregon. (*B*) Tangential section of the tubular sheath of a *Lyngbya*-like oscillatoriacean cyanobacterium in a conical stromatolite (*Conophyton gaubitza*) from the subgreenschist facies 650-Ma-old Chichkan Formation of Kazakstan. (*C*) Transverse cell wall of a broad cellular trichome (*Gunflintia grandis*), and (*D*) a narrow prokaryotic filament (*G. minuta*), in domical stromatolites of the greenschist facies 2,100-Ma-old Gunflint Formation of Ontario, Canada. Each Raman image was produced by combining several hundred pixel-assigned point spectra ("spexels"), like those shown for each specimen in column 3, acquired over a small square part of the total area analyzed. The resolution of the Raman images is defined by the pixel dimensions of their component spexels; for *A*-*C*, 2 µm per pixel, and for *D*, 0.5 µm per pixel.

PNAS

Text and images removed due to copyright restrictions.
Abstract and Fig. 2 in Schopf, J. William, Anatoliy B. Kudryavtsev, David G. Agresti, Thomas J. Wdowiak, and Andrew D. Czaja. "Laser-Raman Imagery of Earth's Earliest Fossils." *Nature* 416 (2002): 73-76.

Text and images removed due to copyright restrictions.

Fig. 3 in Schopf, J. William, Anatoliy B. Kudryavtsev, David G. Agresti, Thomas J. Wdowiak, and Andrew D. Czaja. "Laser-Raman Imagery of Earth's Earliest Fossils." *Nature* 416 (2002): 73-76.

Brief Communications

Nature **420**, 476-477 (5 December 2002) | doi: 10.1038/420476b

Laser−Raman spectroscopy (Communication arising): Images of the Earth's earliest fossils?

Jill Dill Pasteris and Brigitte Wopenka

Abstract

Text removed due to copyright restrictions.
(Abstract of above article).

Astrobiology. 2005
Jun;5(3):333-71.

Raman imagery: a new approach to assess the geochemical maturity and biogenicity of permineralized precambrian fossils.

Schopf JW, Kudryavtsev AB, Agresti DG, Czaja AD, Wdowiak TJ.

Laser-Raman imagery is a non-intrusive, non-destructive analytical technique, recently introduced to Precambrian paleobiology, that can be used to demonstrate a one-to-one spatial correlation between the optically discernible morphology and kerogenous composition of permineralized fossil microorganisms. Made possible by the submicron-scale resolution of the technique and its high sensitivity to the Raman signal of carbonaceous matter, such analyses can be used to determine the chemical-structural characteristics of organic-walled microfossils and associated sapropelic carbonaceous matter in acid-resistant residues and petrographic thin sections. Here we use this technique to analyze kerogenous microscopic fossils and associated carbonaceous sapropel permineralized in 22 unmetamorphosed or little-metamorphosed fine-grained chert units ranging from approximately 400 to approximately 2,100 Ma old.

Astrobiology. 2005
Jun;5(3):333-71.

The lineshapes of the Raman spectra acquired vary systematically with five indices of organic geochemical maturation: (1) the mineral-based metamorphic grade of the fossil-bearing units; (2) the fidelity of preservation of the fossils studied; (3) the color of the organic matter analyzed; and both the (4) H/C and (5) N/C ratios measured in particulate kerogens isolated from bulk samples of the fossil-bearing cherts. Deconvolution of relevant spectra shows that those of relatively well-preserved permineralized kerogens analyzed in situ exhibit a distinctive set of Raman bands that are identifiable also in hydrated organic-walled microfossils and particulate carbonaceous matter freed from the cherts by acid maceration. These distinctive Raman bands, however, become indeterminate upon dehydration of such specimens. To compare quantitatively the variations observed among the spectra measured, we introduce the Raman Index of Preservation, an approximate measure of the geochemical maturity of the kerogens studied that is consistent both with the five indices of organic geochemical alteration and with spectra acquired from fossils experimentally heated under controlled laboratory conditions. The results reported provide new insight into the chemical-structural characteristics of ancient carbonaceous matter, the physicochemical changes that accompany organic geochemical maturation, and a new criterion to be added to the suite of evidence by which to evaluate the origin of minute fossil-like objects of possible but uncertain biogenicity.

Astrobiology. 2005 Jun;5(3):333-71.

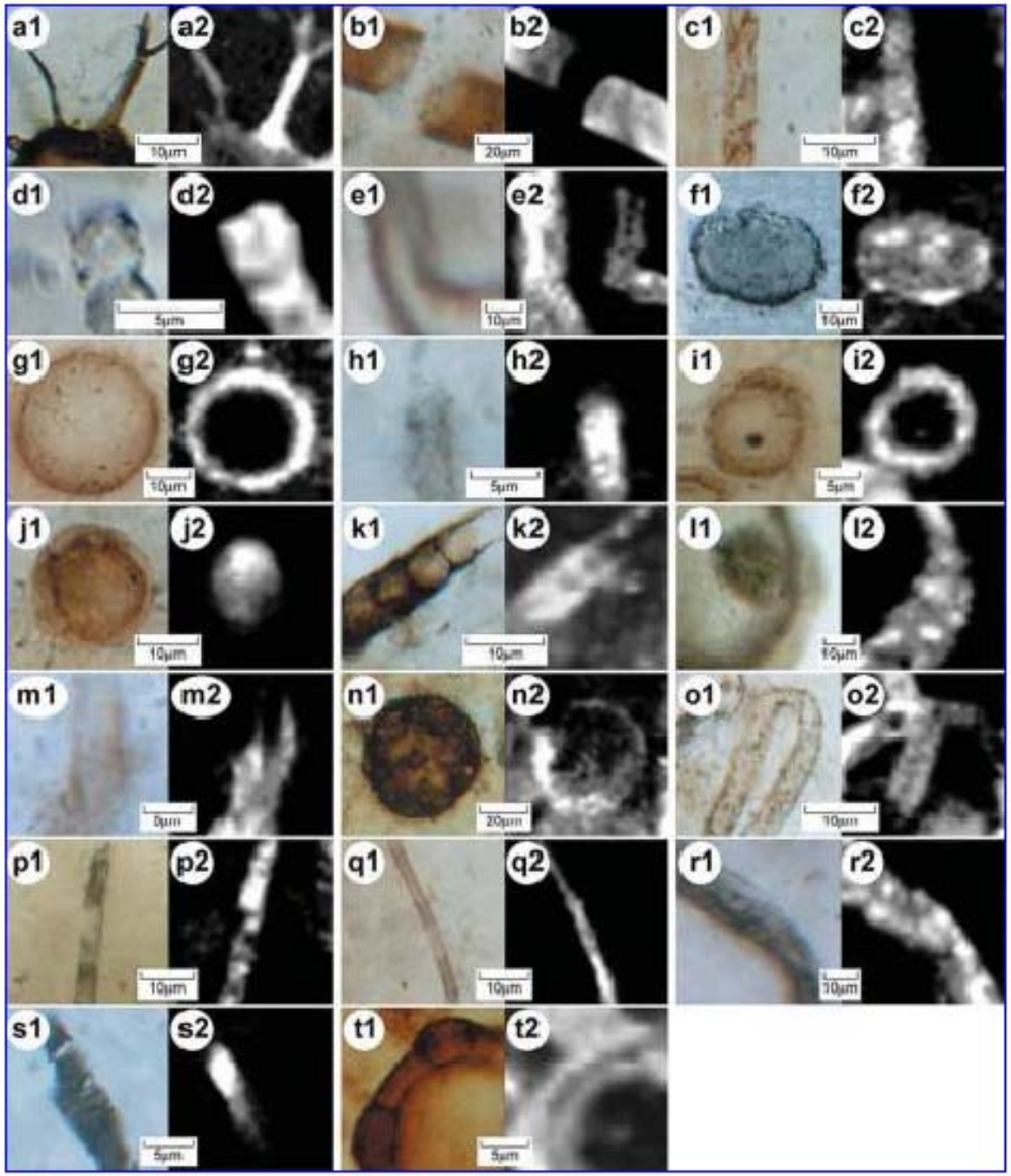

FIG. 4. Areas of the fossils outlined by white rectangles in Fig. 3, shown here in digitized images (denoted by suffix "1") and Raman images of the same areas (denoted by suffix "2"), with the prefix letters indicating the geologic source of the fossils as indicated in Figs. 3 and 9.

Pick the Fossils?

Images removed due to copyright restrictions.

Photographs of real fossils alongside photos of nonliving microstructures that resemble fossils.

Self-Assembled Silica-Carbonate Structures and Detection of Ancient Microfossils

Juan M. Garcia-Ruiz, Stephen T. Hyde, A. M. Carnerup, A. G. Christy, M. J. Van Kranendonk and N. J. Welham

SCIENCE 302, 14 NOVEMBER 2003, 1194-1197

Self-Assembled Silica-Carbonate Structures and Detection of Ancient Microfossils

Juan M. Garcia-Ruiz, Stephen T. Hyde, A. M. Carnerup, A. G. Christy, M. J. Van Kranendonk and N. J. Welham

Image removed due to copyright restrictions.
Figure 2 in Garcia-Ruiz *Science* article.

Fig. 2. Comparison of synthetic filaments with purported ancient microfossils. (**A** to **D**) FESEM images of inorganic in vitro filaments. (A), (B), and (D) As-prepared filaments, containing silica and witherite. [Adapted with permission from (*12*).] (C) Bare barium carbonate (witherite) crystallite aggregate after dissolution of silica in mild alkaline solution. (D) Silica skin, coating the exterior of the aggregates. (**E** and **F**) Microfilaments found in the Warrawoona chert. [(E) Adapted with permission from (*6*); (F) adapted with permission from (*19*).] (**G** to **I**) Optical micrographs of synthetic filaments, showing the progressive dissolution of the solid (witherite) interior of the biomorphs in dilute ethanoic acid, leaving a hollow silica membrane whose morphology is that of the original witherite-silica composite. [Adapted with permission from (*12*).] Scale bars in (A) and (B), 40 μm; in (C), 10 μm; in (D), 4 μm; in (F) to (I), 40 μm [(G) and (I) are at the same magnification as (H)]. A more detailed sequence is available in movie S3.

SCIENCE 302, 14 NOVEMBER 2003, 1194-1197

Self-Assembled Silica-Carbonate Structures and Detection of Ancient Microfossils

Juan M. Garcia-Ruiz, Stephen T. Hyde, A. M. Carnerup, A. G. Christy, M. J. Van Kranendonk and N. J. Welham

SCIENCE 302, 14 NOVEMBER 2003, 1194-1197

Self-Assembled Silica-Carbonate Structures and Detection of Ancient Microfossils

Juan M. Garcia-Ruiz, Stephen T. Hyde, A. M. Carnerup, A. G. Christy, M. J. Van Kranendonk and N. J. Welham

Image removed due to copyright restrictions.
Figure 3 in Garcia-Ruiz *Science* article.

Fig. 3. (**A** to **C**) Optical micrographs of the silica-witherite structure before and after exposure to organic species, all taken under identical illumination. (A) Inorganic structure as prepared. (B) Structure after hydrothermal adsorption of organics. (C) Cured material produced by baking the sample that was preexposed to the organic mixture [as in (B)]. Scale bars, 50 μm. (**D**) (Upper curve) Raman spectrum of heatcured biomorphs (similar to Fig. 3C) compared with kerogen-like Raman spectrum reported by Schopf *et al*. (lower curve), collected from a microfilament in the Archean Warrawoona chert [reproduced with permission from fig. 3H of (*6*)]

SCIENCE 302, 14 NOVEMBER 2003, 1194-1197

3.2 Ga Hyperthermophilic Microbes from W.Aust. Rasmussen 2001

Image removed due to copyright restrictions.

Fig. 3 in Rasmussen, Birger. "Filamentous Microfossils in a 3,235-million-year-old Volcanogenic Massive Sulphide Deposit." *Nature* 405 (2001): 676-679.

Image removed due to copyright restrictions.

Putative cyanobacteria and anaerobic bacteria from the 3.1 Gy Fig Tree Group overlying the Swaziland Group of South Africa.

Image removed due to copyright restrictions.

Barghoorn, E.S. and Tyler, S.A.
1965: Microorganisms from the Gunflint Chert. Science, vol. 147, p. 563-577.

Schopf, J.W.
1999: Cradle of Life: The Discovery of Earth's Earliest Fossils. Princeton University Press, 336 p.

The oldest unequivocal visible remains of a diversity of microorganisms occur in the 2.0 BYO Gunflint Chert of the Canadian Shield

Images removed due to copyright restrictions.

Gunflint Chert Fossils. A-C. blue-green algae; *Animikia, Entosphaeroides,* and *Gunflintia; D. Huroniospora,* an algal spore; *E. Gunflintia* and *Hurionospora; F. Euastrion,* a bacterium, and enigmatic forms, *G. Kakabekia; H. Eosphaera.*

Stromatolites

Images removed due to copyright restrictions.

Photographs of stromatolites. See these examples:
http://upload.wikimedia.org/wikipedia/commons/1/1b/Stromatolites_in_Sharkbay.jpg
http://upload.wikimedia.org/wikipedia/commons/0/02/Lake_Thetis-Stromatolites-LaRuth.jpg

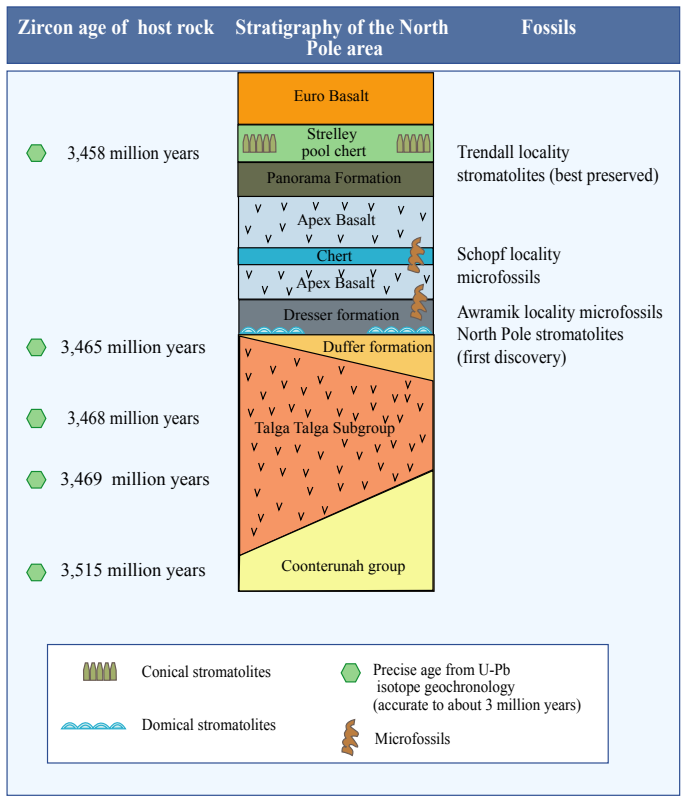

Figure by MIT OpenCourseWare.

Hofmann, H.J., Grey, K., Hickman, A.H., and Thorpe, R. 1999. Origin of 3.45 Ga coniform stromatolites in Warrawoona Group, Western Australia.Geological Society of America, Bulletin, v. 111 (8), p. 1256-1262.

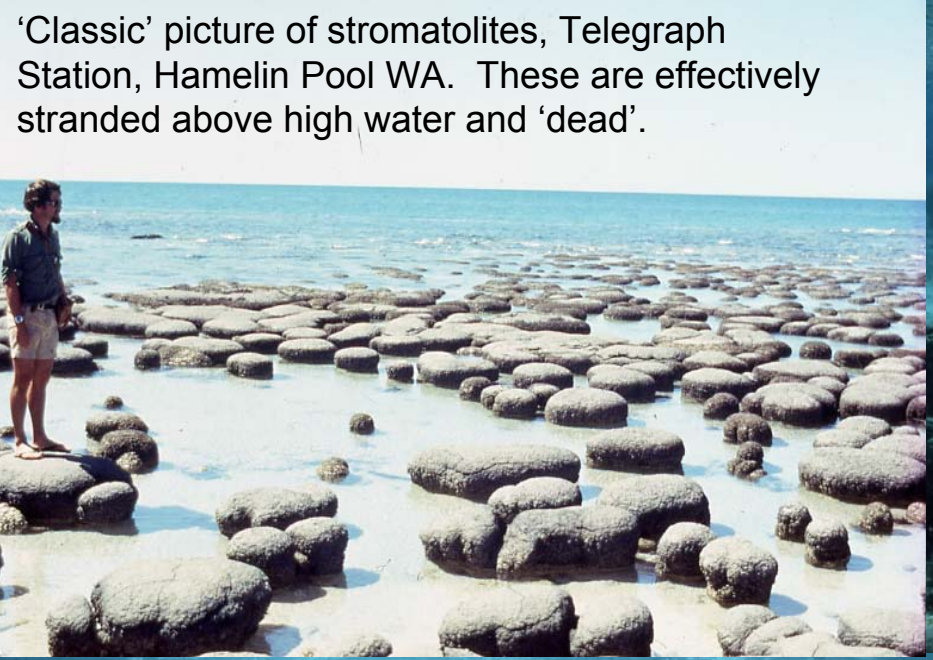

‘Classic’ picture of stromatolites, Telegraph Station, Hamelin Pool WA. These are effectively stranded above high water and ‘dead’.

Small (0.5) club-shaped subtidal stromatolites, Telegraph Station

1m domal subtidal stromatolites, Carbla Point, Hamelin Pool

‘Reef’ of 1m stromatolites, Carbla Point

Examples of 800 million year-old stromatolites from the Officer Basin, Western Australia.

LEFT: *Acaciella australica - a form with narrow columns in bioherms up to 1 metre in diameter.*

ABOVE: *Baicalia burra - a form with broad, irregular branching columns*

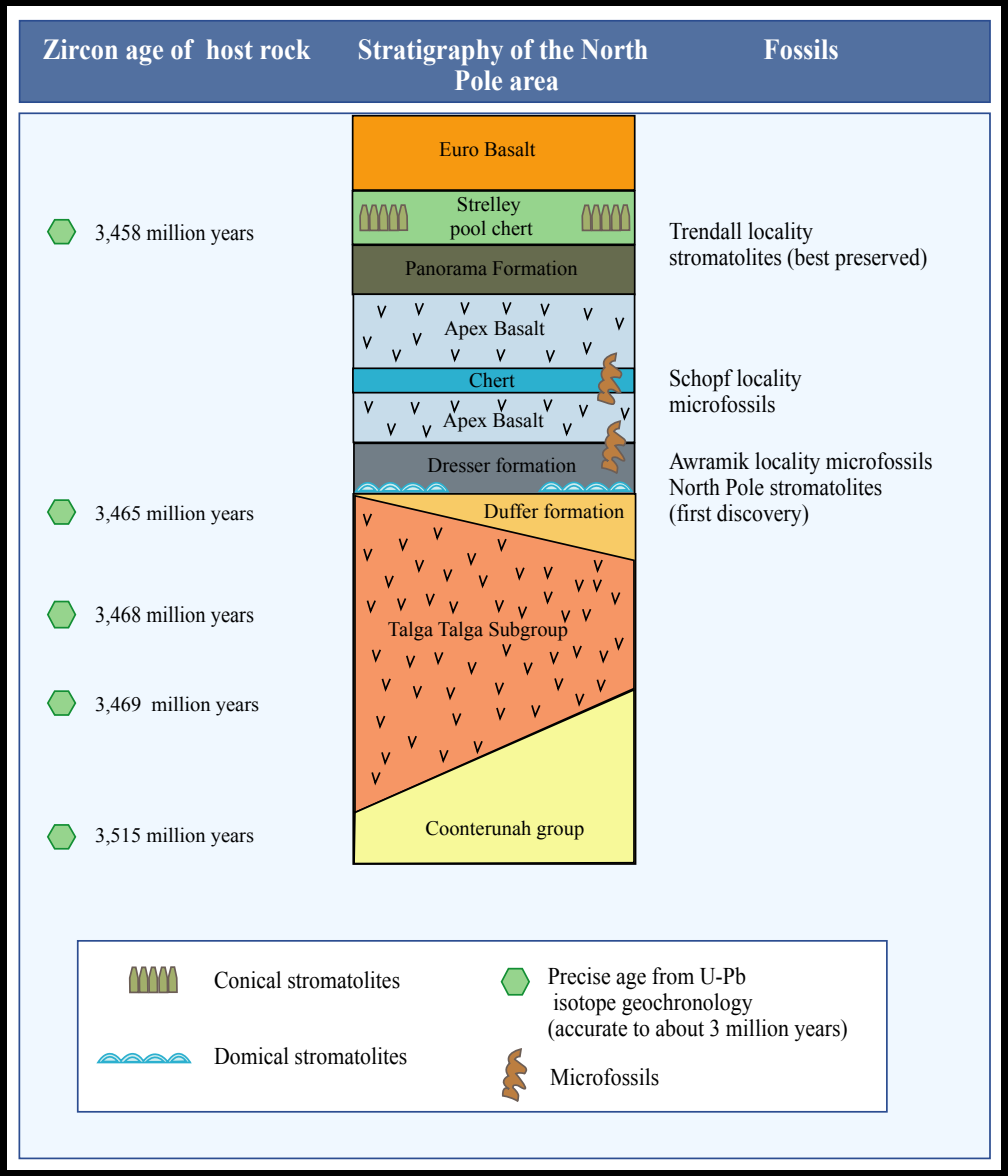

Figure by MIT OpenCourseWare.

Warrawoona Group
3.5-3.4 Ga
volcanics & sediments

Warrawoona Stromatolites Are Perhaps the Oldest Evidence for Life on Earth.

Adapted from TheCarlSaganLecture By Joe Kirschvink
http://www.gps.caltech.edu/users/jkirschvink/

Grotzinger & Knoll ’99
argue that Archean stromatolites could be simple inorganic precipitates!

cones ca 1m high with lensoid laminae

Image removed due to copyright restrictions.

Stromatolite photograph.

RIGHT: *Detail of a branching column formed on the side of a stromatolite cone. Complex structures such as these rule out formation by means such as the folding of soft sediments.*

LEFT: *The outcrop of "egg-carton" stromatolites when first discovered, before removal of the overlying rocks. (Click to enlarge.)*
RIGHT: *The "egg-carton" rock face after the overlying rocks were removed. Although today the "egg-cartons" are tilted at an angle of about 70 degrees, they were originally flat lying.*

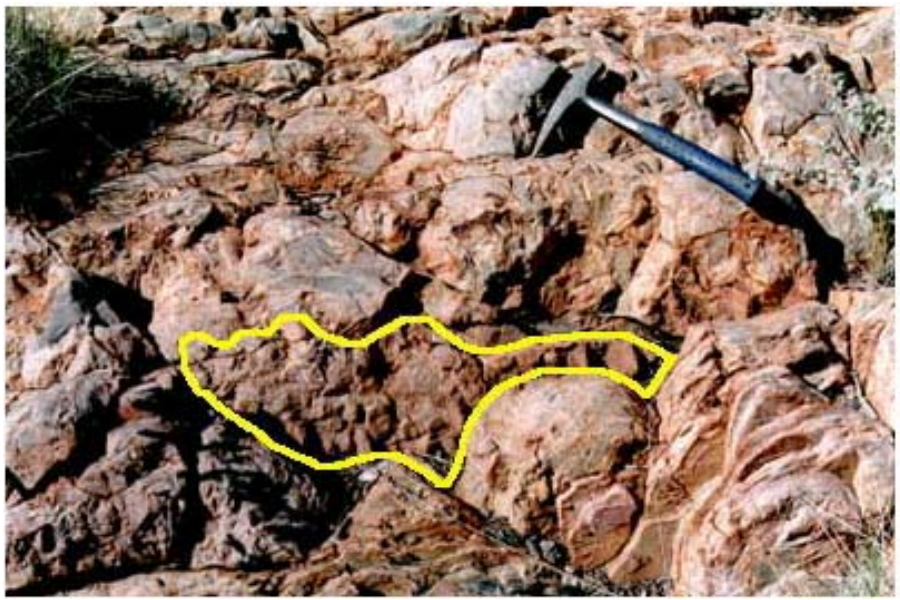

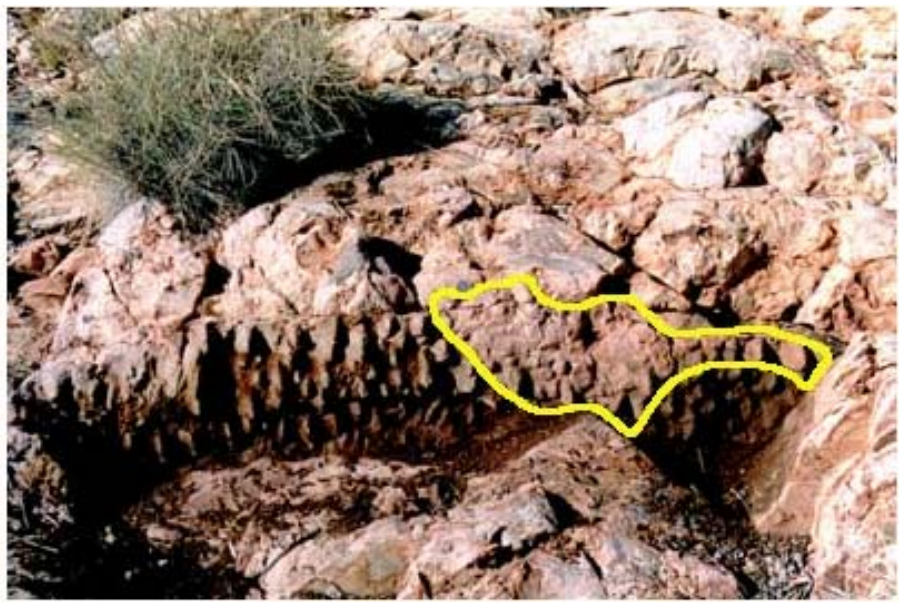

Large Domical Stromatolite
Dresser Fm


Large Dresser Fm dome
from above

Wave ripples
Dresser Fm

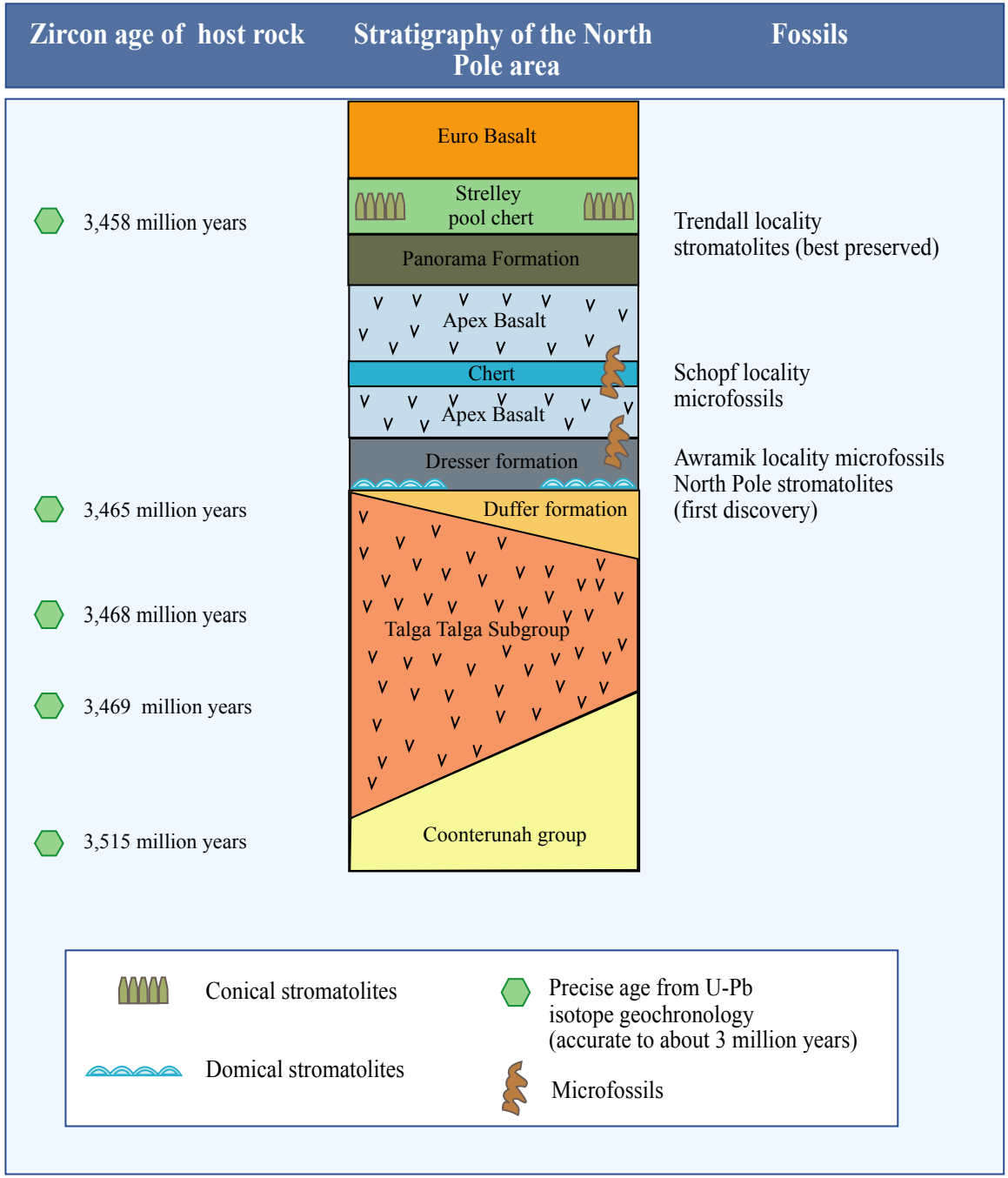

Figure by MIT OpenCourseWare.

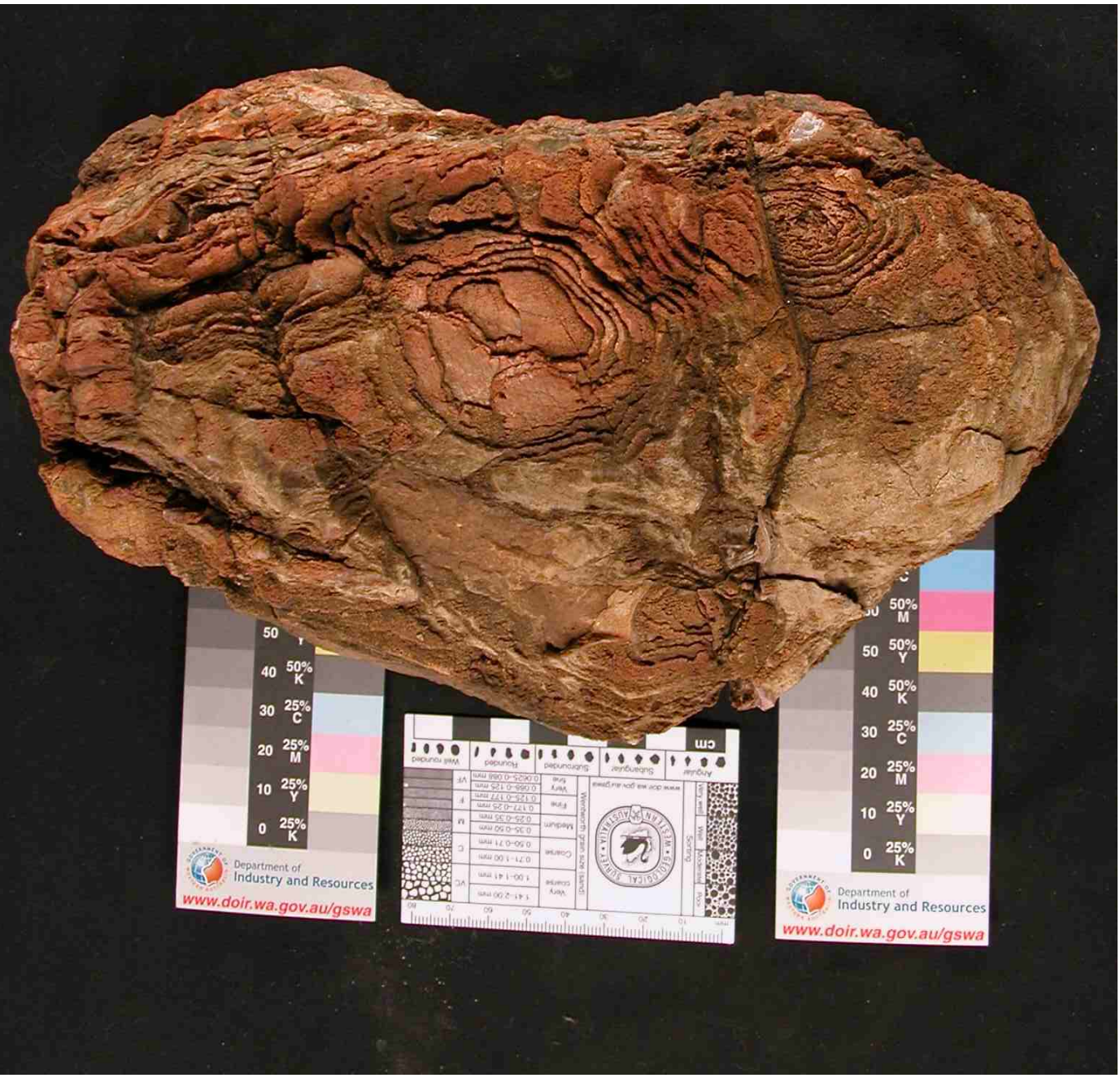
Department of
Industry and Resources
www.doir.wa.gov.au/gswa
Department of
Industry and Resources
www.doir.wa.gov.au/gswa

Oldest Marine Transgression??

Domal stromatolite growing on in situ pebbles of Marble Bar Chert

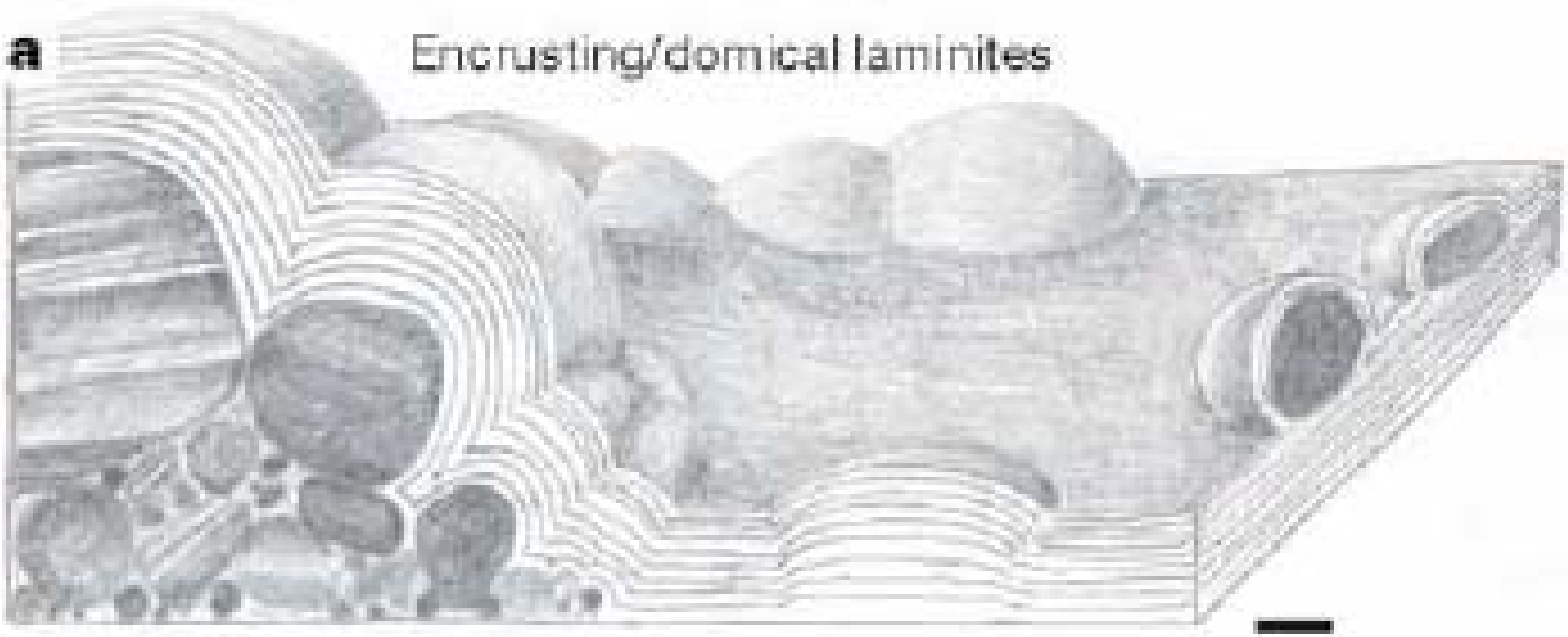

Allwood et al., (2006) Stromatolite reef from the Early Archaean era of Australia. Nature 441|, 714

Mathematical models have ... been used to cast doubt on the biotic origin of stromatolites. Here ... we propose a biotic model for stromatolite morphogenesis which considers the relationship between upward growth of a phototropic or phototactic biofilm (v) and mineral accretion normal to the surface (λ). These processes are sufficient to account for the growth and form of many ancient stomatolites. Domical stromatolites form when $v \leq \lambda$. Coniform structures with thickened apical zones, typical of Conophyton, form when $v >> \lambda$. More angular coniform structures, similar to the stomatolites claimed as the oldest macroscopic evidence of life, form when $v >>>$ lambda.

Abstract of Batchelor, M.T., R.V. Burne, B. I. Henry, M. J. Jackson. "A Case for Biotic Morphogenesis of Coniform Stromatolites." *Physica A* 337 (2004): 319-326.

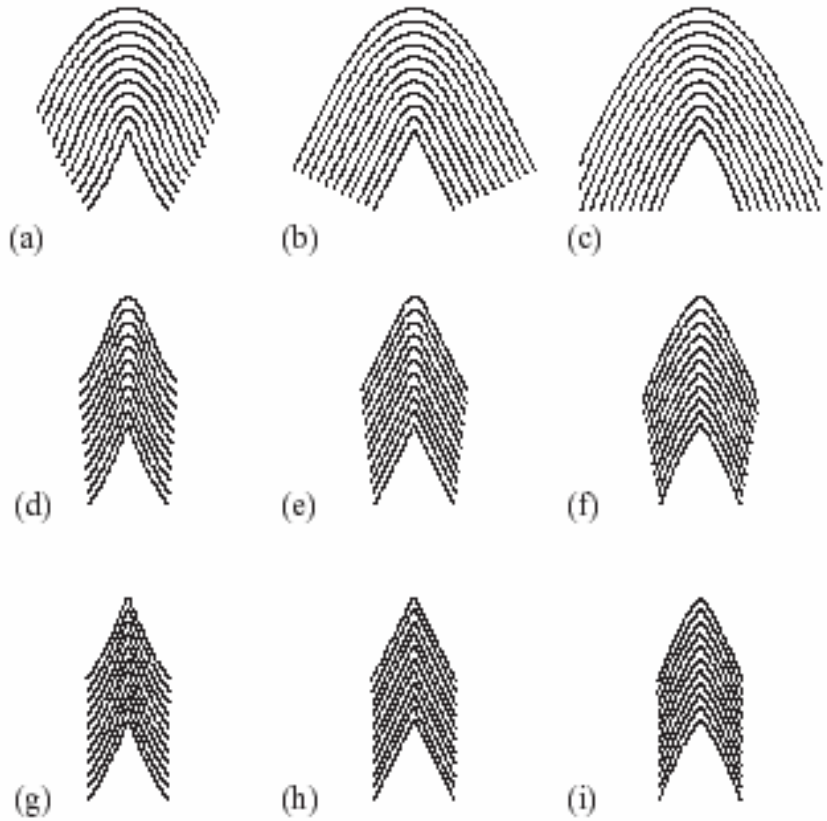

Fig. 1. Equal time snapshots of the surface height profile from the solution of the model, Eqs. (1) and (2), for different values of the initial shape parameters a and α and the growth parameters λ and v. First column: $a = 1.5$, $\alpha = 2$, second column: $a = 0.01$, $\alpha = 2$, third column: $a = -1.5$, $\alpha = 2$. First row: $\lambda = 0.5$, $v = 1$, second row: $\lambda = 0.08$, $v = 1.5$, third row: $\lambda = 0.01$, $v = 1.5$.

Variation modeled by two processes, upward growth and vertical accretion, applied at different rates

Biogeochemical Redox Couples

$CO_2 + H_2O \rightarrow CH_2O + O_2$ oxygenic photosynthesis

Interdependency?

$CH_2O + O_2 \rightarrow CO_2 + H_2O$ aerobic respiration

$CO_2 + 2H_2 \rightarrow CH_4 + 2H_2O$ methanogenesis

$CH_4 + 2O_2 \rightarrow CO_2 + 2H_2O$ oxidative methanotrophy

$CO_2 + HS^- + H_2O \rightarrow \text{biomass} + SO4^{2-}$ anoxygenic photosynthesis

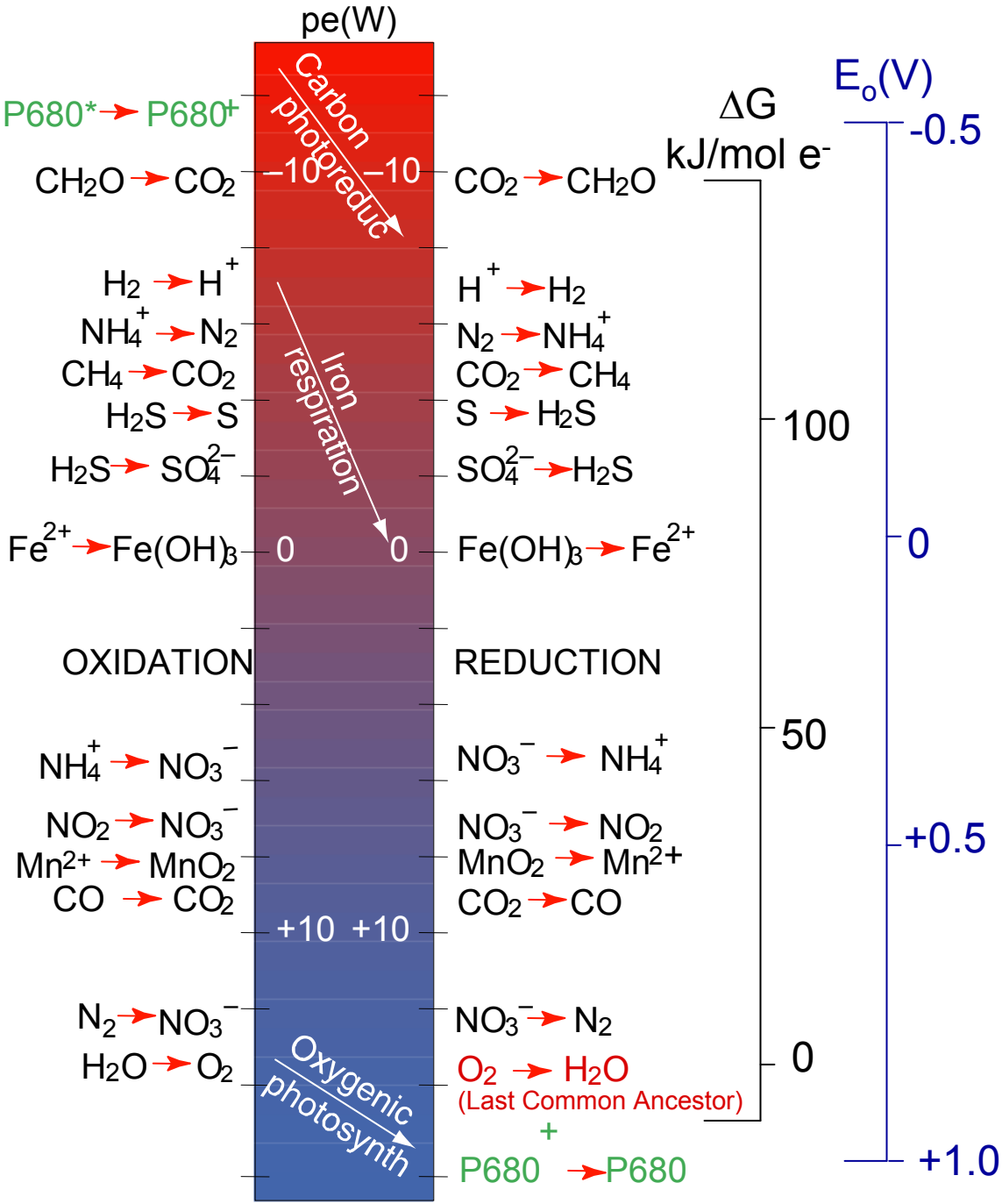

Courtesy of Joe Kirschvink. Used with permission.

Standard Redox Potentials & Energy Yields

The electron tower……..

Strongest reductants, or e donors, on top LHS

Electrons 'fall' until they are 'caught' by available acceptors

The further they fall before being caught, the greater the difference in reduction potential and energy released by the coupled reactions

Note electron fall from CH_2O to O_2 is the among the largest here

$$\Delta G = \Delta G^\circ_{(T)} + RT \cdot \ln K$$

Adapted from TheCarlSaganLecture By Joe Kirschvink
http://www.gps.caltech.edu/users/jkirschvink/

Biogeochemical Redox Couples

aerobic respiration

$$CH_2O + O_2 \rightarrow CO_2 + H_2O$$

1 mole glucose $\xrightarrow{O_2}$ 32 mole ATP

1 mole glucose $\xrightarrow{\text{fermentation}}$ 2-4 mole ATP

Biosynthesis requires approx. 1mole ATP per 4g of cell carbon

Biogeochemical Redox Couples

oxygenic photosynthesis

$$CO_2 + H_2O \rightarrow CH_2O + O_2$$

^{13}C Evidence for Antiquity of Earthly Life

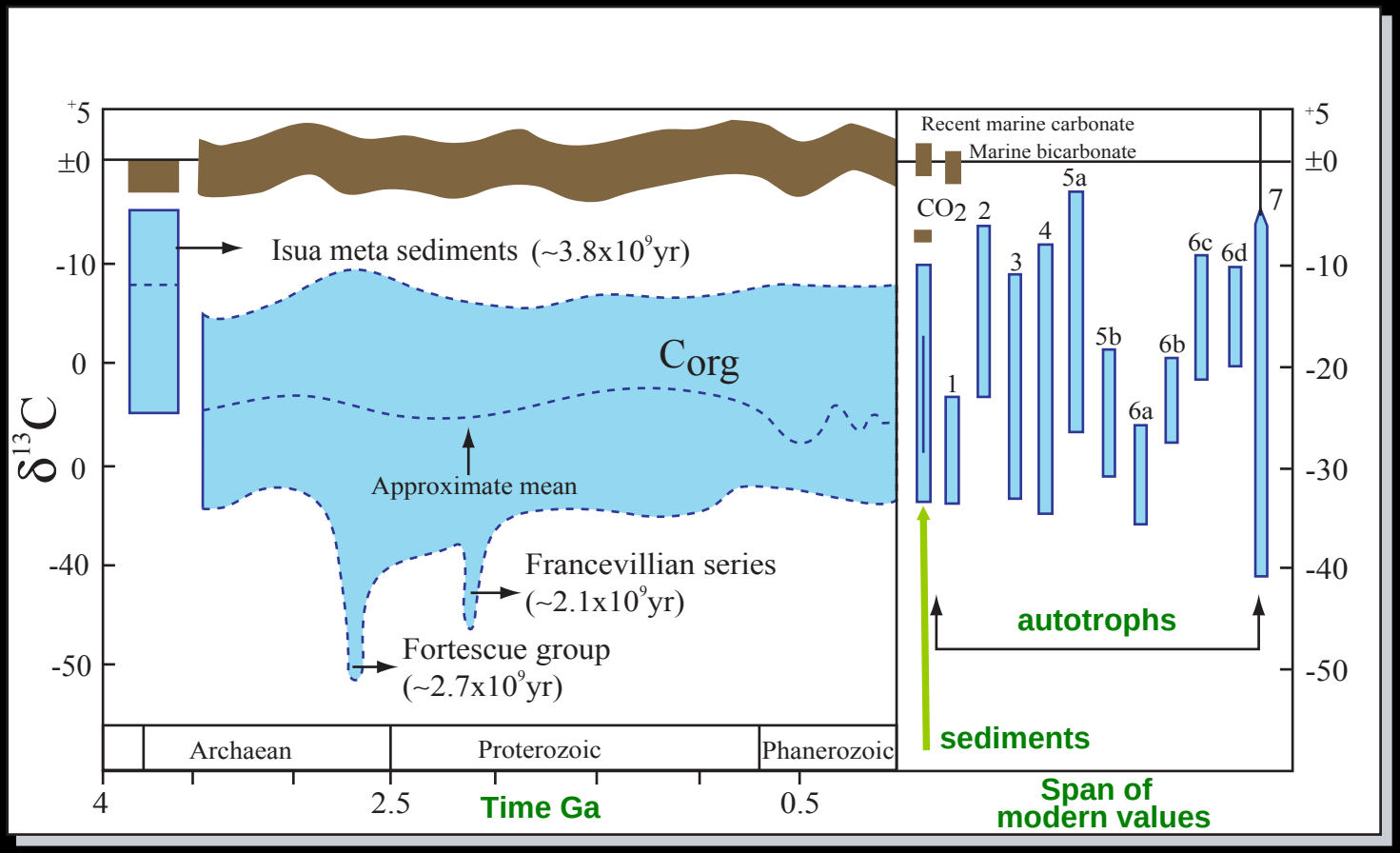

Figure by MIT OpenCourseWare.

Biogeochemical Redox Couples

oxygenic photosynthesis

$$CO_2 + H_2O \rightarrow CH_2O + O_2$$

MINERALISATION THROUGH GEOLOGIC TIME

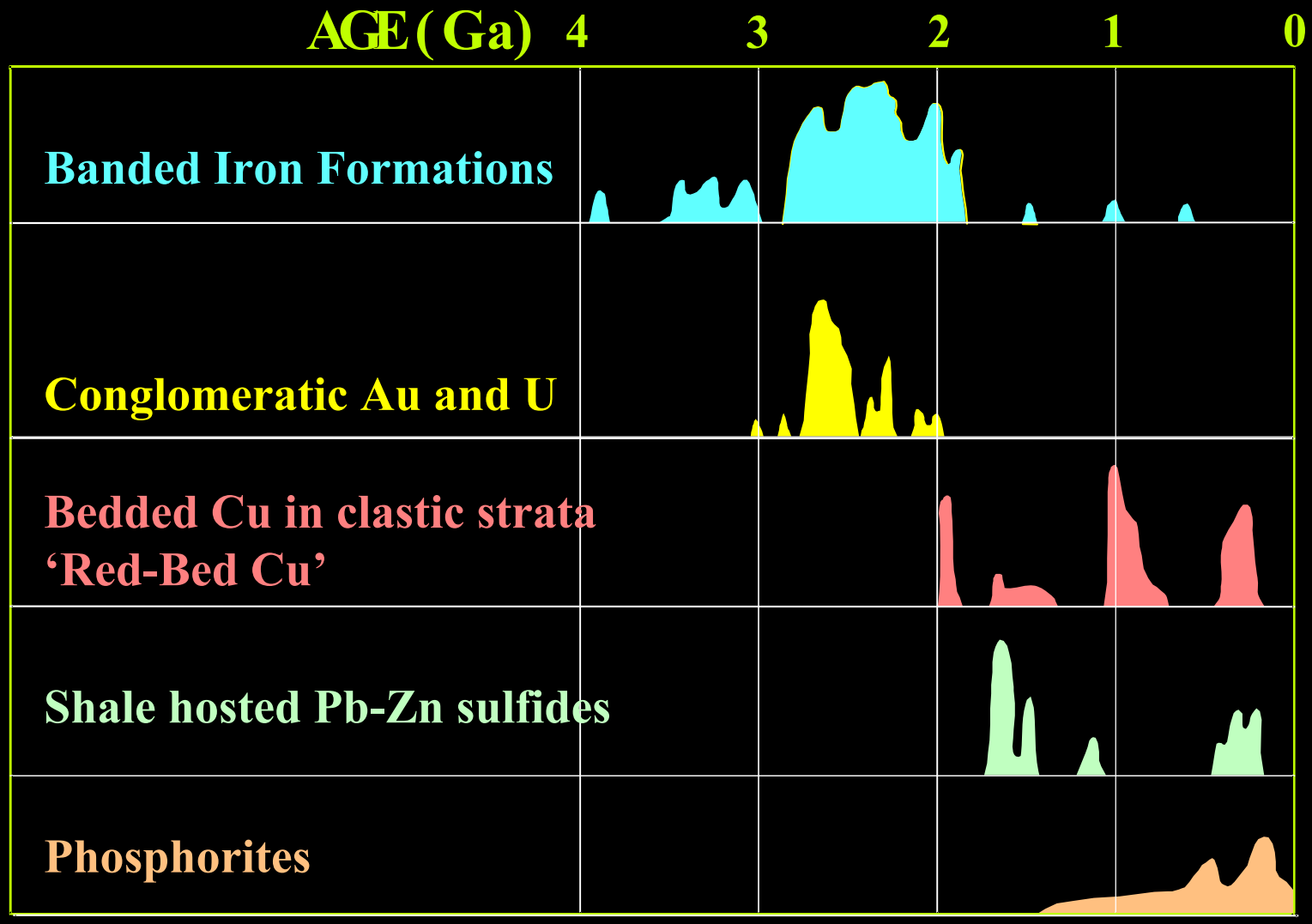

(adapted from Lambert & Groves, 1981)

A Typical Banded Iron Stone (BIF)

Courtesy of Joe Kirschvink. Used with permission.

Precambrian Banded Iron Formations (BIFs) (Adapted from Klein & Beukes, 1992)

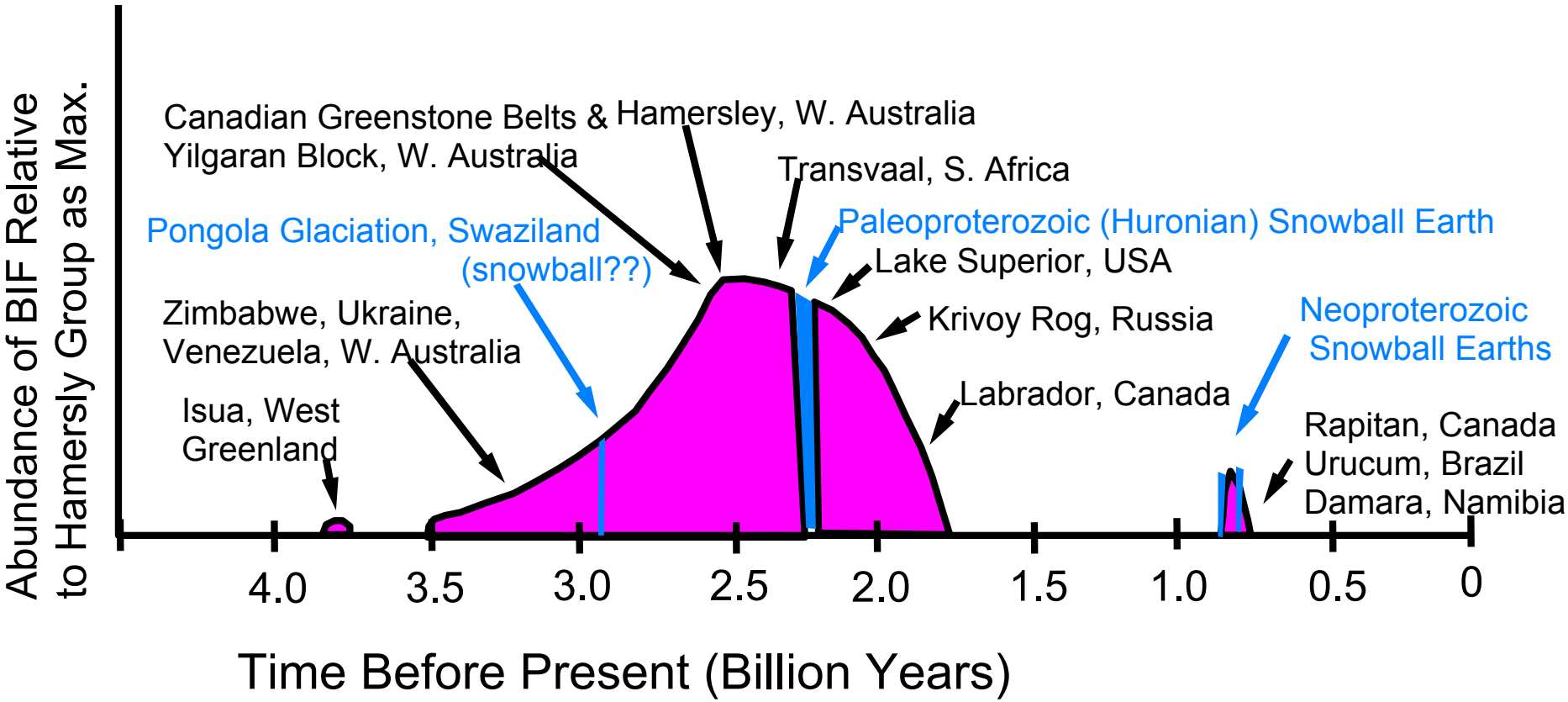

Courtesy Joe Kirschvink, CalTech

Pyrite (FeS_2) is Unstable in O_2-Rich Environments

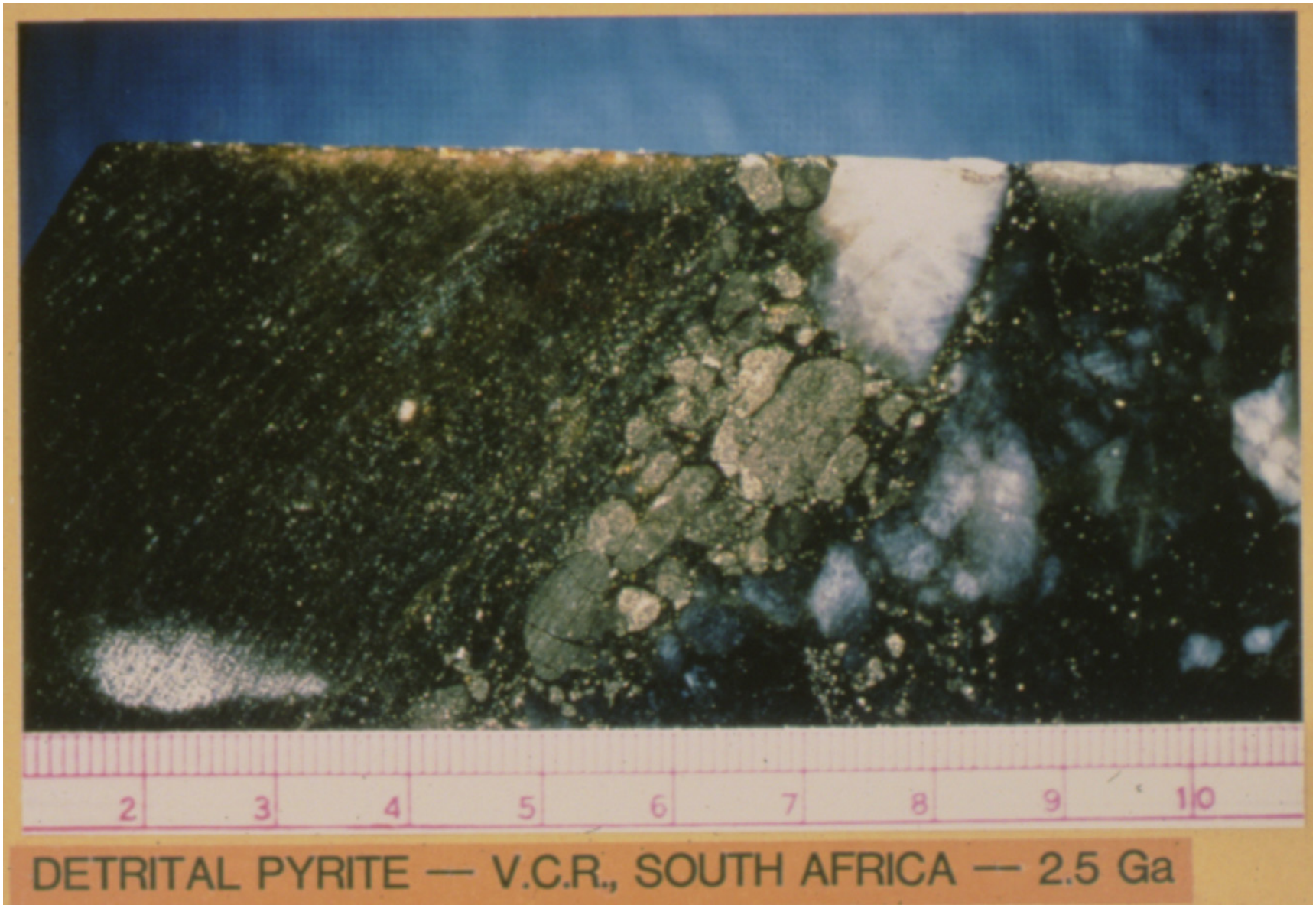

Multicellular Algal Fossils--2.1 Ga

Image removed due to copyright restrictions.

Grypania: genus of coiled multicellular eukaryotic algae.
From 2.1 Ga rocks in Michigan.

Stanley (1999)

Likely sequence of critical evolutionary events leading to multicellular forms

Image removed due to copyright restrictions.

- Eukaryotes likely arose from union of two prokaryotic cells.
- Internalized cell became mitochondrion (where E from food derived by respiration).
- DNA & RNA in mitochondrion is different than in surrounding cells.
- Protozoan consumed & retained cyanobacterium that became chloroplast.
- Chloroplasts contain own DNA & RNA (like mitochonrdrion) and are remarkably similar to cyanobacteria.

Stanley (1999)

Life's History on Earth

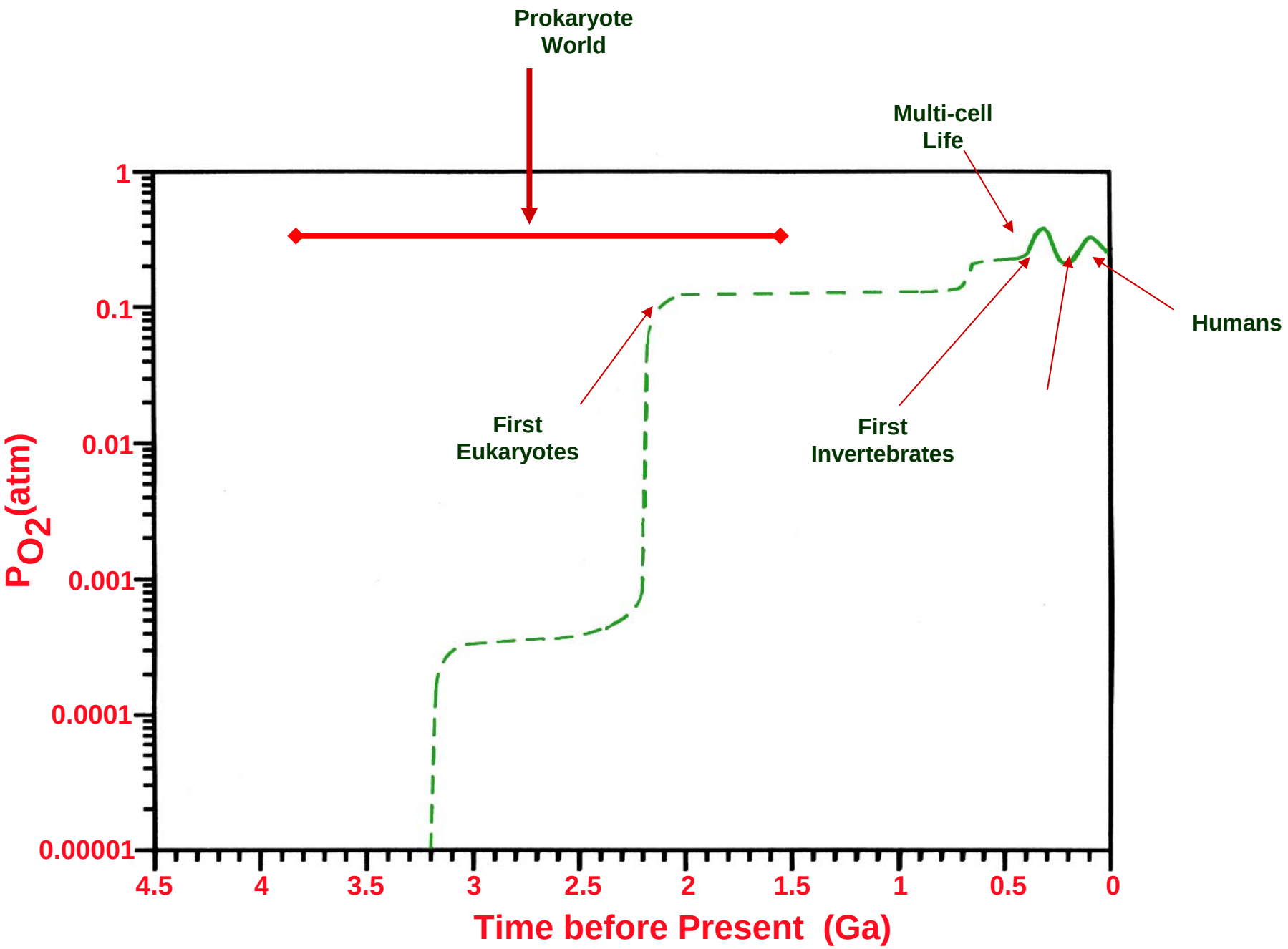

Images removed due to copyright restrictions.

Steroids and O_2

Jahnke & Klein 1983 showed epoxidase synthesis stimulated at 0.03% (c. 300nM)

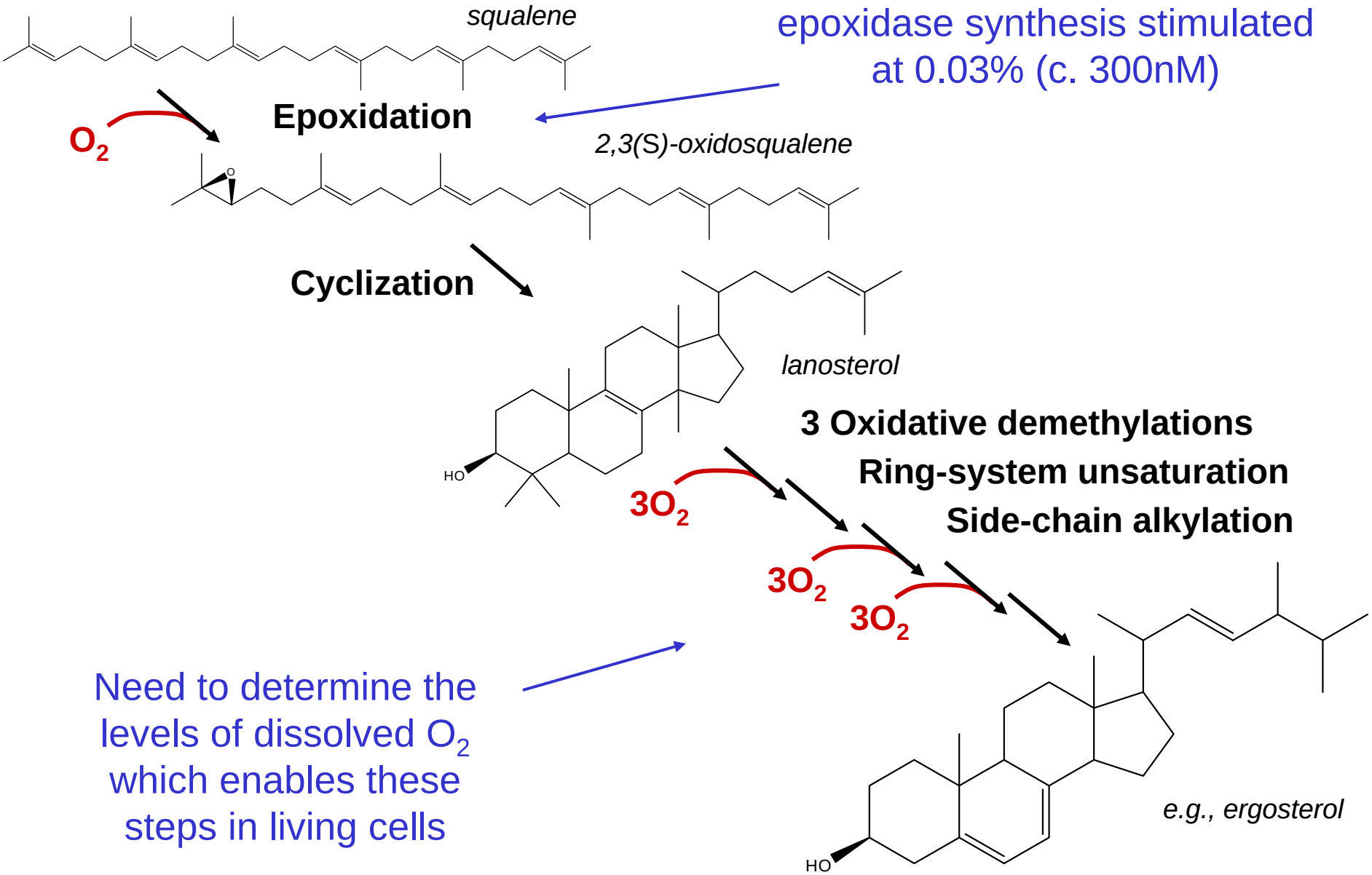

Need to determine the levels of dissolved O_2 which enables these steps in living cells

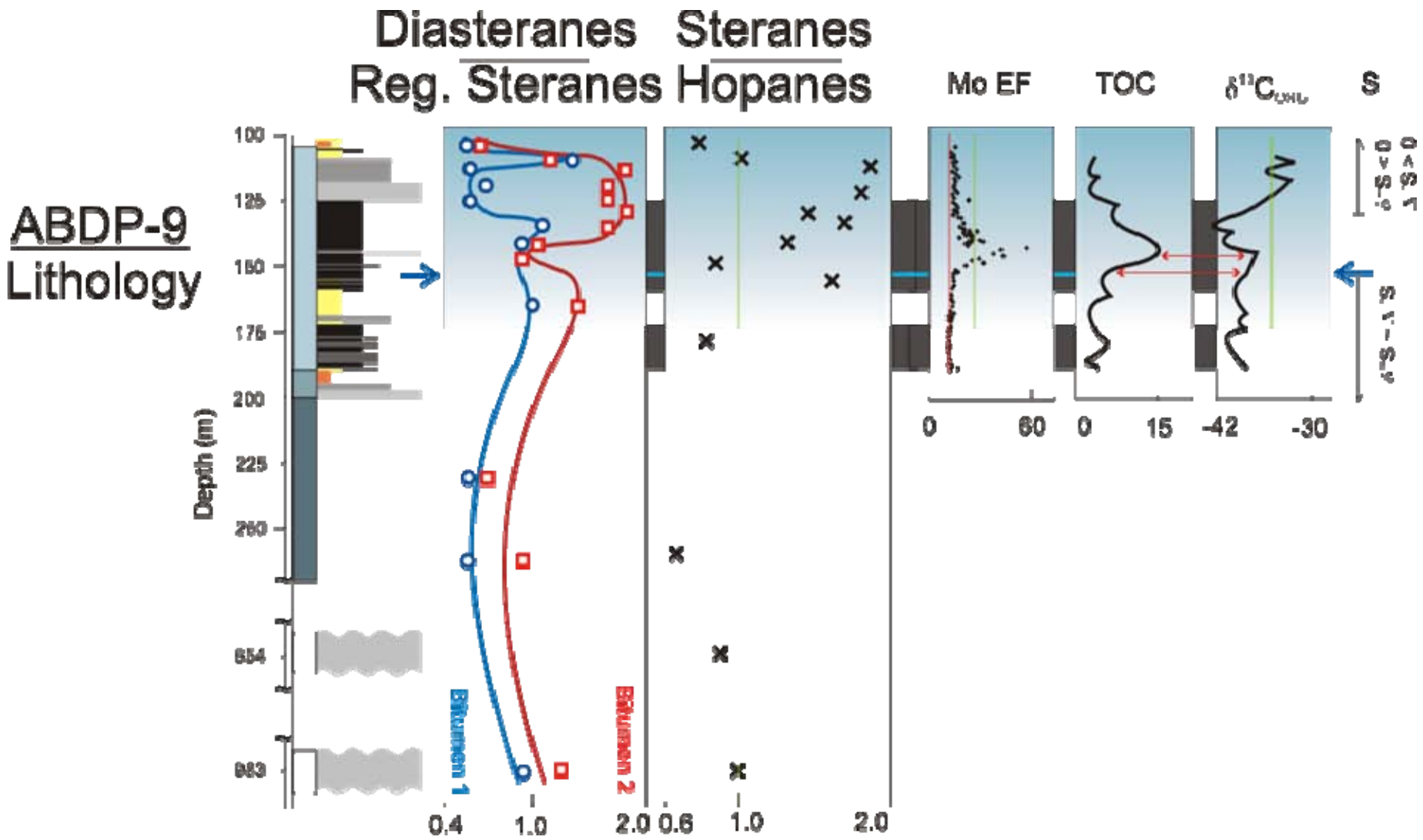
ABDP-9
Lithology
Diasteranes
Reg. Steranes
Steranes
Hopanes
Mo EF
TOC
δ13C
S
Depth (m)
100
125
150
175
200
225
250
654
983
Bitumen 1
Bitumen 2
0.4
1.0
2.0
0.6
1.0
2.0
0
60
0
15
-42
-30
δ34S < 0
Δ33S > 0
δ34S > 1‰

Bitumen 2

Multiple sulfur isotopes

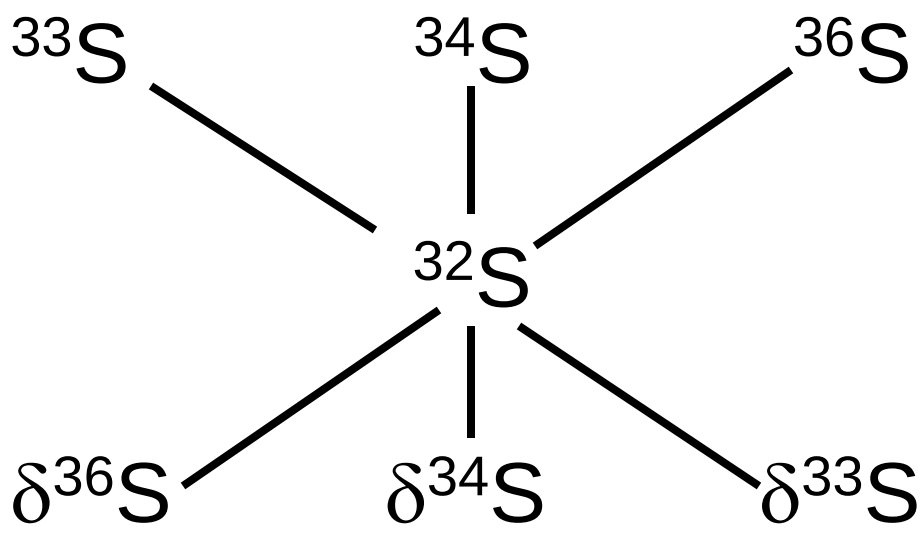

Mass-dependent Fractionation:

$\delta^{33}S=0.515\delta^{34}S$, $\delta^{36}S=1.91\delta^{34}S$

Sulfur Isotopic Evidence for O_2 -#2

Atmospheric Influence of Earth's Earliest Sulfur Cycle

James Farquhar,* Huiming Bao, Mark Thiemens

Mass-independent isotopic signatures for $\delta^{33}S$, $\delta^{34}S$, and $\delta^{36}S$ from sulfide and sulfate in Precambrian rocks indicate that a change occurred in the sulfur cycle between 2090 and 2450 million years ago (Ma). Before 2450 Ma, the cycle was influenced by gas-phase atmospheric reactions. These atmospheric reactions also played a role in determining the oxidation state of sulfur, implying that atmospheric oxygen partial pressures were low and that the roles of oxidative weathering and of microbial oxidation and reduction of sulfur were minimal. Atmospheric fractionation processes should be considered in the use of sulfur isotopes to study the onset and consequences of microbial fractionation processes in Earth's early history.

Images removed due to copyright restrictions.

Kasting (2001) *Science* **293**:819-820; J. Farquhar, H. Bao, M. Thiemens (2000) *Science* **289**:756-758.

Mass Independent Fractionation

ELSEVIER

Available online at www.sciencedirect.com

SCIENCE DIRECT®

Earth and Planetary Science Letters 213 (2003) 15–30

EPSL

www.elsevier.com/locate/epsl

New insights into Archean sulfur cycle from mass-independent sulfur isotope records from the Hamersley Basin, Australia

Shuhei Ono[a,*], Jennifer L. Eigenbrode[b], Alexander A. Pavlov[c], Pushker Kharecha[b], Douglas Rumble III[a], James F. Kasting[b], Katherine H. Freeman[b]

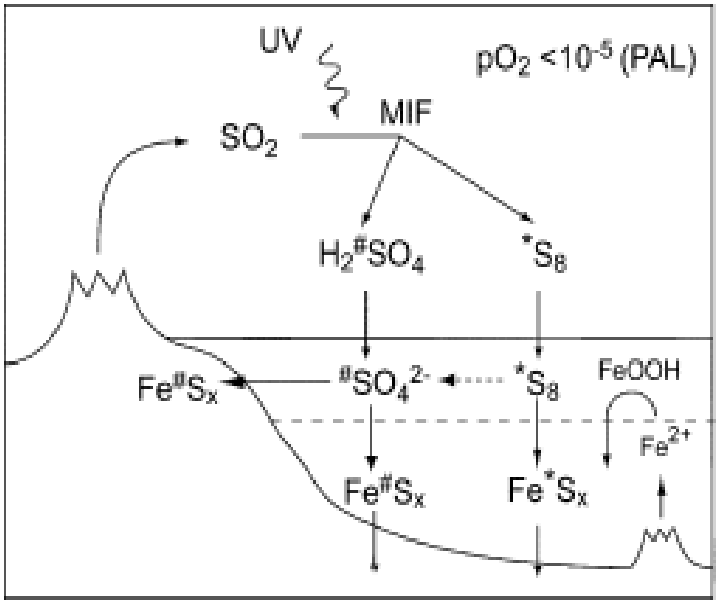

Fig. 3. A conceptual model of Archean sulfur cycle. Photochemistry in the atmosphere causes MIF in sulfur isotopes, and aerosols of S_8 and H_2SO_4 carry sulfur with positive (*S) and negative (#S) v33S signatures, respectively. The preservation of MIF signatures in the sediments implies incomplete oxidation of S8 in the ocean (dashed arrow).

Mass Independent Fractionation

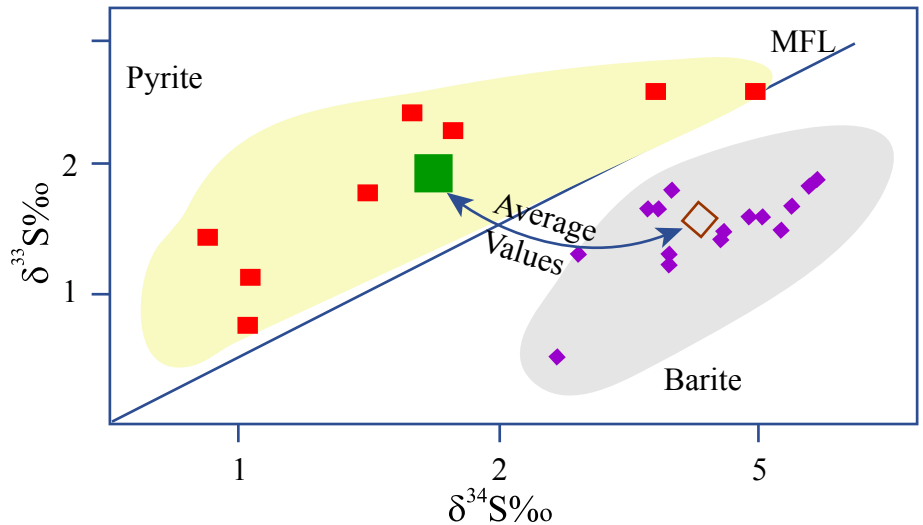

Data from 3.3-3.5 Ga sedimentary sulfides and sulfates. All Phanerozoic sulfides and sulfates plot along the MFL line.

Figure by MIT OpenCourseWare. After Farquhar et al., 2001.

Mass-Independent Fractionation of Sulfur Isotopes in Archean Sediments: Strong Evidence for an Anoxic Archean Atmosphere

A.A. PAVLOV and J.F. KASTING **ASTROBIOLOGY Volume 2, Number 1, 2002**

Sulfur Isotopic Evidence for O_2

Image removed due to copyright restrictions.

J. Farquhar, H. Bao, M. Thiemens (2000) *Science* **289**:756-758.

Conundrum: If oxygen-producing photosynthesis was occurring by 3.5-2.7 Ga, why doesn't free O_2 appear until 2.3 Ga, a 1200-400 Myr delay?

The BIG question in geobiology today!!

Conundrum: If oxygen-producing photosynthesis was occurring by 3.5-2.7 Ga, why doesn't free O2 appear until 2.3 Ga, a 1200-400 Myr delay?

Sources

- Photosynthesis
- Hydrogen escape

Vs.

Sinks

- Respiration
- Reduced minerals in rocks
- Reduced volcanic gases
- Reduced hydrothermal vent fluids